Precipitation, radiative forcing and global temperature change

Timothy Andrews,[1] Piers M. Forster,[1] Olivier Boucher,[2] Nicolas Bellouin,[2] and Andy Jones[2]

[1] Radiative forcing is a useful tool for predicting equilibrium global temperature change. However, it is not so useful for predicting global precipitation changes, as changes in precipitation strongly depend on the climate change mechanism and how it perturbs the atmospheric and surface energy budgets. Here a suite of climate model experiments and radiative transfer calculations are used to quantify and assess this dependency across a range of climate change mechanisms. It is shown that the precipitation response can be split into two parts: a fast atmospheric response that strongly correlates with the atmospheric component of radiative forcing, and a slower response to global surface temperature change that is independent of the climate change mechanism, ~2-3% per unit of global surface temperature change. We highlight the precipitation response to black carbon aerosol forcing as falling within this range despite having an equilibrium response that is of opposite sign to the radiative forcing and global temperature change. **Citation:** Andrews, T., P. M. Forster, O. Boucher, N. Bellouin, and A. Jones (2010), Precipitation, radiative forcing and global temperature change, *Geophys. Res. Lett.*, *37*, L14701, doi:10.1029/2010GL043991.

1. Introduction

[2] Radiative forcing is a useful concept for predicting equilibrium changes in global surface-air-temperature, ΔT. It is quantified by the near-instantaneous change in the Earth's energy balance caused by a climate change mechanism, as measured at the top-of-atmosphere (TOA) or tropopause. However, radiative forcing is not such a useful tool for predicting changes in global precipitation, ΔP. This is because precipitation changes are more constrained by the atmospheric and surface energy budgets [e.g., *Boer*, 1993; *Allen and Ingram*, 2002; *Stephens and Ellis*, 2008; *Takahashi*, 2009; *Lambert and Allen*, 2009], rather than energy budget changes at the TOA or tropopause.

[3] Different climate change mechanisms perturb the TOA, atmospheric and surface energy budgets in different ways. For example aerosols have a large impact on the surface and/or atmospheric energy balance as they can both scatter and absorb solar radiation in the atmosphere. Aerosols are therefore expected to play an important role in perturbing the Earth's hydrological cycle [e.g., *Ramanathan et al.*, 2001]. The impact of a climate change mechanism on precipitation is often quantified by the hydrological sensitivity, defined as the change in precipitation per unit of ΔT, which is generally larger under solar forcings than under greenhouse-gas forcings [e.g., *Feichter et al.*, 2004; *Liepert and Previdi*, 2009]. Moreover under black carbon aerosol forcing the hydrological sensitivity can be negative [*Jones et al.*, 2007], hence even the sign of the precipitation change does not necessarily depend on the sign of the radiative forcing or ΔT.

[4] The reason the hydrological sensitivity varies across different climate change mechanisms is not because precipitation is responding differently to ΔT, but because, as we will show, precipitation also responds to the change in atmospheric radiative heating caused by the presence of the forcing agent. While this has been shown to be true for CO_2 and solar forcings [*Lambert and Faull*, 2007; *Andrews et al.*, 2009; *Bala et al.*, 2009] it is the purpose of this article to quantify and assess how robust this is across a range of different climate change mechanisms, including different greenhouse-gases, ozone and solar output changes, different aerosols species and a change in the albedo of snow. Furthermore, we aim to quantify the relationship between radiative forcing, its partitioning between the atmosphere and surface, and precipitation changes.

2. Experiments and Method

2.1. Model Setup

[5] We use an atmospheric model based on the Hadley Centre climate model HadGEM1 [*Martin et al.*, 2006] with various improvements coupled to a 50 m thermodynamic mixed-layer ocean and sea-ice model (see *Jones et al.* [2007] for further description of the improvements and base configuration of the model). A mixed-layer ocean model is a simplification of the climate system, however, *Takahashi* [2009] found the hydrological sensitivities of CMIP3 models to be representative of their fully dynamic ocean model counterparts. Nine different forcing scenarios (Table 1) have been integrated from a control simulation based on pre-industrial (year 1860) conditions. The nine forcing scenarios were integrated for 10-years in atmosphere-only mode (i.e., using prescribed sea-surface-temperatures (SSTs) and sea-ice extent) and 30-years in the full atmosphere/mixed-layer mode.

2.2. Method: Fast, Slow and Total Responses

[6] Precipitation can respond to both changes in ΔT and to the forcing agent itself. The direct response to the forcing agent can be demonstrated in forcing experiments with SSTs held fixed (as ΔT is largely prohibited). For example when CO_2 is increased but SSTs held fixed, the precipitation and evaporation rate go down [e.g., *Yang et al.*, 2003; *Dong et al.*, 2009; *Bala et al.*, 2009] due to small increases in tropospheric

---

[1]Institute for Climate and Atmospheric Science, School of Earth and Environment, University of Leeds, Leeds, UK.
[2]Met Office Hadley Centre, Exeter, UK.

Table 1. Description of the Forcing Scenarios[a]

Forcing Scenario	Description
CO_2	CO_2 concentration increased to 2005 levels (286 → 379 ppmv)
$2 \times CO_2$	CO_2 concentration doubled (286 → 572 ppmv)
CH_4	CH_4 concentration increased to 2005 levels (805 → 1,774 ppbv)
Snow albedo	Land snow albedo decreased from 0.80 to 0.75[b]
Solar	Solar constant increased by 2% (1365 → 1392.3 Wm^{-2})
O_3	Tropospheric and stratospheric O_3 changed to 1990 levels
SO_4	SO_2 emissions changed from 1860 to year 2000[c]
BB	Biomass burning emissions changed from 1860 to year 2000[c]
BC	Black carbon emissions changed from 1860 to year 2000[c]

[a]The base configuration of the model uses greenhouse gas concentrations and aerosol emissions representative of the year 1860.
[b]See *Bellouin and Boucher* [2010] for further description.
[c]See *Jones et al.* [2007] for further description.

temperatures above an unchanged surface, increasing atmospheric stability and reducing convection [*Dong et al.*, 2009]. In addition to this response, precipitation also responds to ΔT, through various climate feedbacks that affect precipitation processes, climate models suggest this to be ~ 2–3% K^{-1} [*Held and Soden*, 2006; *Lambert and Webb*, 2008]. These two responses emerge on different timescales due to the smaller heat capacity of the atmosphere compared to the ocean: for example, in response to increased CO_2 the precipitation rate initially goes down due to the direct atmospheric response, before subsequently increasing on a multi-annual timescale associated with ΔT [e.g., *Yang et al.*, 2003; *Andrews et al.*, 2009; *Bala et al.*, 2009]. We refer to these precipitation responses as the "fast," ΔP_{fast}, and "slow," ΔP_{slow}, responses, respectively.

[7] To quantify the ΔP_{fast} and ΔP_{slow} terms we follow the method put forward by *Bala et al.* [2009]. The total change in any climate variable x is the sum of the fast and slow responses, $\Delta x_{total} = \Delta x_{fast} + \Delta x_{slow}$. The total change is simply the change in the full atmosphere/mixed-layer integrations, from which we discard the first 10-years (the transient part) and calculate equilibrium responses from the average of the remaining 20-years. The fast component is determined from the atmosphere-only integrations where ΔT is largely prohibited; we average over all 10-years. We calculate the slow response from subtracting the fast response from the total response [see *Bala et al.*, 2009]. Note that fast and slow responses can also be estimated from linear regression during transient climate change [*Gregory and Webb*, 2008], which can also provide useful energetic constraints on how much precipitation increases with ΔT [e.g., *Takahashi*, 2009], but is inappropriate here as the transient change (ΔT) is not large enough in most of our experiments to constrain the regression lines.

[8] In the following analysis the reported error in any term x is calculated from Monte Carlo simulations. We randomly sample an equal number of annual-means from the original dataset to create 10,000 subsets, and then compute the required term x from each of these sets. The 95% uncertainty

in x is then determined from the standard deviation of the 10,000 simulated x values.

2.3. Radiative Forcing Calculations

[9] For CO_2, CH_4, O_3 and the solar experiment, radiative forcings are calculated offline using the Edwards-Slingo radiation code [*Edwards and Slingo*, 1996]. We take the difference between two calls of the radiation code, one based on the control configuration and one with the forcing agent introduced. The influence of stratospheric adjustment is accounted for using the fixed-dynamical-heating approximation [*Forster et al.*, 1997]. For black carbon (BC) aerosol it is important to resolve high-frequency temporal variations because the relative position of cloud and aerosols are important. Therefore, the radiative forcing is calculated online by running a 5-year simulation with the model in atmosphere-only mode. As with the offline calculations, the radiation code is called twice, the call based on the control configuration is passed on to the next model time step. The snow albedo forcing is calculated similarly [see *Bellouin and Boucher*, 2010]. As SO_4 and biomass burning (BB) aerosol act as cloud condensation nuclei in the model these radiative forcings are calculated from the change in radiation balance in the fixed-SST experiments, which allows the aerosol indirect effects to be incorporated into the forcing estimate [e.g., *Lohmann et al.*, 2010]. Note that as stratospheric adjustment is accounted for (or is negligible for the black carbon and snow albedo forcing) the radiative forcing at the TOA and tropopause is the same, hence any atmospheric forcing only remains in the troposphere.

3. Results

[10] The fast, slow and total precipitation responses are shown in Table 2. To compare across the forcing scenarios, we normalise the total precipitation response by total surface-
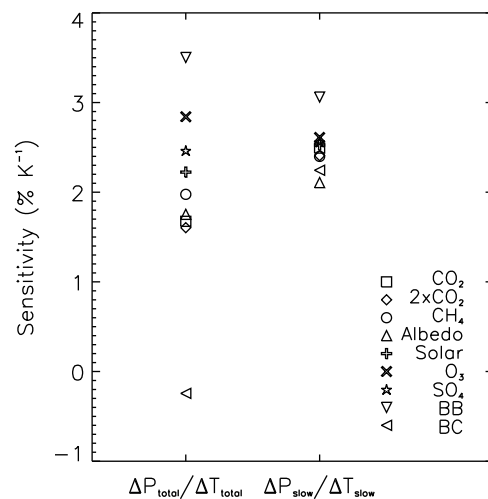
Figure 1. Comparison of the hydrological sensitivity ($\Delta P/\Delta T$) for a standard method that just considers the total responses only (left), and a method that considers only the slow components of climate change (right). The apparent dependence of the hydrological sensitivity on the forcing agent is largely removed if the fast precipitation response is removed.

Table 2. The Fast, Slow and Total Precipitation Responses[a]

Forcing Scenario	ΔP_{fast} (%)	ΔP_{slow} (%)	ΔP_{total} (%)	$\Delta P_{total}/\Delta T_{total}$ (% K^{-1})	$\Delta P_{slow}/\Delta T_{slow}$ (% K^{-1})
CO_2	-1.12 ± 0.14	3.67 ± 0.23	2.55 ± 0.18	1.68 ± 0.10	2.49 ± 0.14
$2 \times CO_2$	-2.53 ± 0.18	8.71 ± 0.26	6.18 ± 0.18	1.60 ± 0.03	2.41 ± 0.06
CH_4	-0.21 ± 0.23	1.30 ± 0.32	1.09 ± 0.22	1.98 ± 0.52	2.40 ± 0.86
Snow albedo	-0.04 ± 0.19	1.30 ± 0.24	1.26 ± 0.14	1.75 ± 0.18	2.11 ± 0.37
Solar	-0.91 ± 0.17	10.23 ± 0.27	9.31 ± 0.21	2.22 ± 0.04	2.53 ± 0.06
O_3	0.02 ± 0.17	0.53 ± 0.23	0.55 ± 0.15	2.84 ± 0.83	2.61 ± 1.44
SO_4	0.03 ± 0.13	-2.90 ± 0.19	-2.87 ± 0.13	2.46 ± 0.11	2.56 ± 0.16
BB	-0.18 ± 0.19	-0.57 ± 0.24	-0.75 ± 0.14	3.50 ± 0.74	3.06 ± 1.05
BC	-0.68 ± 0.18	0.61 ± 0.26	-0.07 ± 0.19	-0.24 ± 0.72	2.25 ± 0.87

[a]Fast, ΔP_{fast}; slow, ΔP_{slow}; total, $\Delta P_{total} = \Delta P_{fast} + \Delta P_{slow}$. Also shown is the hydrological sensitivity ($\Delta P/\Delta T$) for i) standard methods that do not separate fast and slow responses ($\Delta P_{total}/\Delta T_{total}$), and, ii) for the slow responses only ($\Delta P_{slow}/\Delta T_{slow}$). Errors represent 95% uncertainties.

air-temperature change (fifth column in Table 2). This "hydrological sensitivity" is seen to vary considerably across the forcing mechanisms (range is -0.24 to $+3.5\%$ K^{-1}), recovering the result of previous studies that precipitation changes strongly depend on the nature of the forcing mechanism. However, if we compute the hydrological sensitivity for only the slow components of climate change (that is, the component that scales with ΔT), we find a hydrological sensitivity (sixth column in Table 2) that is now in good agreement across the forcing agents; in all experiments the slow precipitation response to ΔT is of the order 2–3% K^{-1}. Previously this has had only been shown for the case of CO_2 and solar forcing [*Lambert and Faull*, 2007; *Andrews et al.*, 2009; *Bala et al.*, 2009]; our results show it to be a robust result across a range of climate change mechanisms. The comparison is illustrated in Figure 1. It is notable that even black carbon aerosol, which had a negative hydrological sensitivity, falls within the 2–3% K^{-1} range when only the slow components of climate change are considered.

[11] To further understand the fast and slow precipitation responses we examine the link between precipitation changes and radiative forcing as measured at the TOA, F_{toa}, and its partitioning between the surface, F_{srf}, and atmosphere, F_{atm}. Table 3 shows the radiative forcing terms and the ratio $R = F_{srf}/F_{toa}$. For climate change mechanisms that force climate through the scattering of solar radiation, such as SO_4 and snow albedo, or changes in the solar constant, R is close to unity, indicating that the atmosphere is largely transparent to these forcings, which are felt at the surface. Black carbon aerosol strongly absorbs solar radiation in the atmosphere, which reduces solar radiation reaching the surface (F_{srf} is

negative) but also reduces outgoing solar radiation to space (F_{toa} is positive). Therefore the surface radiative forcing is of opposite sign to the radiative forcing at the TOA [e.g., *Ramanathan et al.*, 2001], as seen in Table 3 where $R = -1.5$. Biomass burning aerosol both scatters, which generates a negative radiative forcing at the TOA and surface, and absorbs solar radiation, which generates a small positive atmospheric component, therefore $R > 1$. O_3 radiative forcing is more complex due to competing effects in the solar and thermal spectra, as well as competing increases and decreases in concentration through the troposphere and stratosphere. The net global-mean effect is an R close to unity. The radiative forcing of both CO_2 and CH_4 increases with height throughout the troposphere [*Collins et al.*, 2006], hence it is mostly absorbed in the atmosphere and $R < 1$.

[12] We test which components of radiative forcing are a good predictor for the fast and slow precipitation responses in Figure 2. Figure 2 (left) shows the relationship between the fast precipitation response and radiative forcing across the experiments. F_{toa} and F_{srf} appear to be bad predictors of ΔP_{fast} (Figures 2a and 2c), while the correlation between F_{atm} and ΔP_{fast} (Figure 2e) is excellent. The reason F_{atm} correlates so well with ΔP_{fast} can be understood from energetic grounds [e.g., *Allen and Ingram*, 2002]. Radiative cooling of the atmosphere is balanced by latent heating (precipitation) and sensible heating. Assuming small changes in sensible heating and tropospheric temperatures, any perturbation to the atmospheric radiative cooling (e.g., F_{atm}) is balanced by a change in precipitation. We test how good this model is in Table 3, where the fast responses in surface latent and sensible heat fluxes are shown (ΔLH and ΔSH,

Table 3. Radiative Forcing at the Top-of-Atmosphere and Its Partitioning Between the Surface and Atmosphere[a]

Forcing Scenario	F_{toa}	F_{srf}	F_{atm}	$R = F_{srf}/F_{toa}$	ΔLH	ΔSH
CO_2	1.39	0.28	1.11	0.2	1.02 ± 0.13	0.01 ± 0.06
$2 \times CO_2$	3.47	0.66	2.81	0.2	2.30 ± 0.18	0.14 ± 0.05
CH_4	0.51	0.26	0.25	0.5	0.18 ± 0.21	0.07 ± 0.07
Snow albedo	0.28	0.29	-0.02	1.0	0.02 ± 0.18	-0.06 ± 0.06
Solar	4.86	3.7	1.16	0.8	0.84 ± 0.16	-0.08 ± 0.07
O_3	0.16	0.21	-0.05	1.3	-0.02 ± 0.15	-0.06 ± 0.05
SO_4	-1.15	-1.17	0.01	1.0	-0.03 ± 0.13	0.05 ± 0.06
BB	-0.29	-0.54	0.25	1.9	0.16 ± 0.17	0.09 ± 0.04
BC	0.36	-0.54	0.90	-1.5	0.62 ± 0.18	0.20 ± 0.05

[a]F, radiative forcing; toa, top-of-atmosphere; srf, surface; atm, atmosphere. R is the ratio of surface radiative forcing over top-of-atmosphere radiative forcing. The fast response in latent heat (ΔLH) and sensible heat (ΔSH) fluxes is also shown. All fluxes are defined as positive downwards. Units are Wm^{-2} except for R which is dimensionless. Errors in the response terms represent 95% uncertainties.
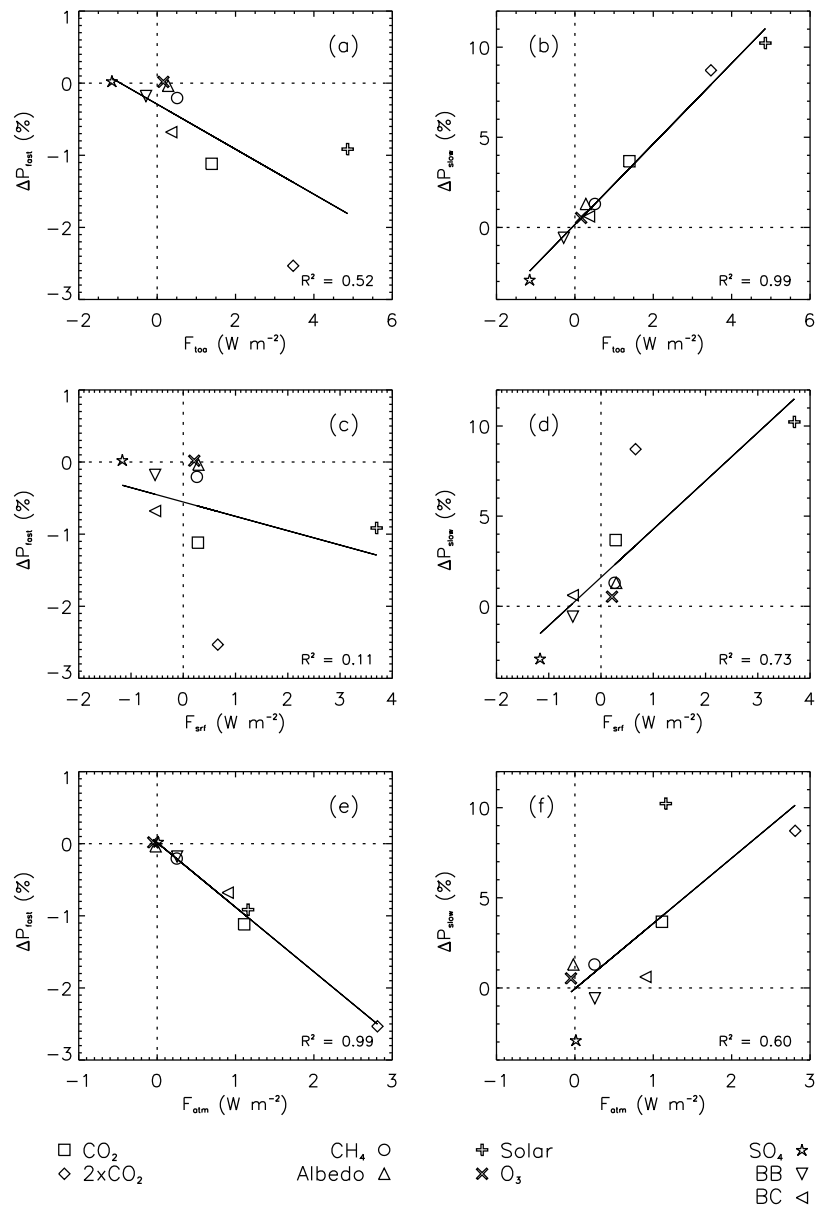
Figure 2. Relationship between (a and b) radiative forcing (F_{toa}), its partitioning between (c and d) the surface (F_{srf}) and (e and f) the atmosphere (F_{atm}), and (left) the fast precipitation response (ΔP_{fast}) and (right) the slow precipitation response (ΔP_{slow}). Symbols represent the different forcing scenarios.

respectively). F_{atm} does appear to be largely balanced by ΔLH, and ΔSH is small. However, in general the sum of ΔLH and ΔSH is not large enough to meet F_{atm} exactly. This is expected: it is the result of small changes in atmospheric temperatures that act to radiate away some of F_{atm}. Changes in temperature are required as a physical mechanism to change ΔLH and ΔSH, as well as other possible factors such as changes in clouds [e.g., *Gregory and Webb*, 2008; *Andrews and Forster*, 2008].

[13] We further note that the residual between F_{atm} and the sum of ΔLH and ΔSH is slightly larger for the solar forcing than CO_2, despite them having a similar F_{atm} component (Table 3). This supports the findings of *Lambert and Faull* [2007] that the atmospheric component of solar radiative forcings is balanced more by atmospheric warming than precipitation changes, compared to a CO_2 scenario. A thorough explanation would require a detailed analysis of the physical mechanisms, but our central point still holds, that is, the dominant term in eliminating F_{atm} is a change in precipitation (even for solar forcings (Table 3)).

[14] Figure 2 (right) shows the relationship between the slow precipitation response and components of radiative forcing across the experiments. F_{toa} is an excellent predictor of ΔP_{slow} (Figure 2b), while F_{srf} and F_{atm} are relatively poor predictors (Figures 2d and 2f). The correlation between F_{toa} and ΔP_{slow} is simply an expression of the radiative forcing concept, i.e., ΔP_{slow} scales with ΔT which can be predicted from the radiative forcing.

4. Conclusions and Discussion

[15] We have examined the precipitation response to a range of climate change mechanisms and quantified its

relationship to radiative forcing, including its partitioning between the atmosphere and surface. By distinguishing two different timescale responses, a quick atmospheric response to the forcing and a slower response to global temperature change, we have shown that the apparent forcing dependence of the hydrological sensitivity stems from a fast atmospheric response (see Figure 1). The fast response correlates extremely well with the amount of radiative forcing absorbed in the atmosphere, suggesting that the fast precipitation changes are a mechanism in which the atmosphere regains its energy balance. In all the experiments the subsequent response of precipitation to global surface–air–temperature change is ~ 2–3% K^{-1} and can be predicted from the radiative forcing as measured at the tropopause or TOA (assuming a sensitivity).

[16] These results improve our understanding of precipitation changes and its relationship to radiative forcing. For example, it shows that climate change mechanisms that largely force climate through the scattering of solar radiation, such as SO_4 and snow albedo, or changes in the solar constant, largely perturb precipitation through changes in global surface temperature which can be predicted through traditional radiative forcing calculations. On the other hand, climate change mechanisms that significantly force climate through absorption of radiation in the troposphere, such as greenhouse gases and black carbon aerosol, have opposing impacts on the precipitation, which require a partitioning of the radiative forcing between the surface and atmosphere to be predicted. In most cases the response to global surface temperature change dominates. However, for black carbon aerosol, the atmospheric component of radiative forcing is sufficiently large that the precipitation response may be of opposite sign to the radiative forcing and global surface temperature change.

[17] We encourage other modelling groups to perform similar experiments to check the robustness of these results. In particular, it has been suggested that fast responses may emerge on different timescales in climate models with full-ocean dynamics compared to their mixed-layer counterparts [*Williams et al.*, 2008]. Nevertheless, our model results have practical applications to real world observations and climate predictions. For example, observed estimates of the hydrological sensitivity are not in fact measuring the true precipitation response to global temperature change, they are measuring the fast and slow precipitation responses as they evolve together. Therefore observed estimates of the hydrological sensitivity are likely to change in the future as forcings change and should not be used to project hydrological cycle changes into the future. Our findings offer the opportunity to improve simple climate models used to extrapolate more complex climate models to multiple climate change scenarios. We suggest that observations and projections of precipitation changes will be aided by expanding the radiative forcing concept to include the atmospheric and surface energy budgets, as highlighted here and by the *National Research Council* [2005].

References

Allen, M. R., and W. J. Ingram (2002), Constraints on future changes in climate and the hydrological cycle, *Nature*, *419*, 224–232, doi:10.1038/nature01092.

Andrews, T., and P. M. Forster (2008), CO_2 forcing induces semi-direct effects with consequences for climate feedback interpretations, *Geophys. Res. Lett.*, *35*, L04802, doi:10.1029/2007GL032273.

Andrews, T., P. M. Forster, and J. M. Gregory (2009), A surface energy perspective on climate change, *J. Clim.*, *22*, 2557–2570, doi:10.1175/2008JCLI2759.1.

Bala, G., K. Caldeira, and R. Nemani (2009), Fast versus slow response in climate change: implications for the global hydrological cycle, *Clim. Dyn.*, doi:10.1007/s00382-009-0583-y.

Bellouin, N., and O. Boucher (2010), Climate response and efficacy of snow albedo forcing in the HadGEM2-AML climate model, *Tech. Note 82*, Met Off. Hadley Cent., Exeter, U. K.

Boer, G. J. (1993), Climate change and the regulation of the surface moisture and energy budgets, *Clim. Dyn.*, *8*, 225–239, doi:10.1007/BF00198617.

Collins, W. D., et al. (2006), Radiative forcing by well-mixed greenhouse gases: Estimates from climate models in the IPCC AR4, *J. Geophys. Res.*, *111*, D14317, doi:10.1029/2005JD006713.

Dong, B., J. M. Gregory, and R. T. Sutton (2009), Understanding land-sea warming contrast in response to increasing greenhouse gases. Part I: Transient adjustment, *J. Clim.*, *22*, 3079–3097, doi:10.1175/2009JCLI2652.1.

Edwards, J., and A. Slingo (1996), Studies with a flexible new radiation code. I: Choosing a configuration for a large-scale model, *Q. J. R. Meteorol. Soc.*, *122*, 689–719, doi:10.1002/qj.49712253107.

Feichter, J., E. Roeckner, U. Lohmann, and B. Liepert (2004), Nonlinear aspects of the climate response to greenhouse gas and aerosol forcing, *J. Clim.*, *17*, 2384–2398, doi:10.1175/1520-0442(2004)017<2384:NAOTCR>2.0.CO;2.

Forster, P. M., R. S. Freckleton, and K. P. Shine (1997), On aspects of the concept of radiative forcing, *Clim. Dyn.*, *13*, 547–560, doi:10.1007/s003820050182.

Gregory, J. M., and M. Webb (2008), Tropospheric adjustment induces a cloud component in CO_2 forcing, *J. Clim.*, *21*, 58–71, doi:10.1175/2007JCLI1834.1.

Held, I. M., and B. J. Soden (2006), Robust responses of the hydrological cycle to global warming, *J. Clim.*, *19*, 5686–5699, doi:10.1175/JCLI3990.1.

Jones, A., J. M. Haywood, and O. Boucher (2007), Aerosol forcing, climate response and climate sensitivity in the Hadley Centre climate model, *J. Geophys. Res.*, *112*, D20211, doi:10.1029/2007JD008688.

Lambert, F. H., and M. R. Allen (2009), Are changes in global precipitation constrained by the tropospheric energy budget?, *J. Clim.*, *22*, 499–517, doi:10.1175/2008JCLI2135.1.

Lambert, F. H., and N. E. Faull (2007), Tropospheric adjustment: The response of two general circulation models to a change in insolation, *Geophys. Res. Lett.*, *34*, L03701, doi:10.1029/2006GL028124.

Lambert, F. H., and M. J. Webb (2008), Dependency of global mean precipitation on surface temperature, *Geophys. Res. Lett.*, *35*, L16706, doi:10.1029/2008GL034838.

Liepert, B. G., and M. Previdi (2009), Do models and observations disagree on the rainfall response to global warming?, *J. Clim.*, *22*, 3156–3166, doi:10.1175/2008JCLI2472.1.

Lohmann, U., et al. (2010), Total aerosol effect: Radiative forcing or radiative flux perturbation?, *Atmos. Chem. Phys.*, *10*, 3235–3246, doi:10.5194/acp-10-3235-2010.

Martin, G. M., M. A. Ringer, V. D. Pope, A. Jones, C. Dearden, and T. J. Hinton (2006), The physical properties of the atmosphere in the new Hadley Centre Global Environmental Model (HadGEM1). Part I: Model description and global climatology, *J. Clim.*, *19*, 1274–1301, doi:10.1175/JCLI3636.1.

National Research Council (2005), *Radiative Forcing of Climate Change*, 207 pp., National Acad. Press, Washington, D. C.

Ramanathan, V., P. J. Crutzen, J. T. Kiehl, and D. Rosenfeld (2001), Aerosols, climate, and the hydrological cycle, *Science*, *294*, 2119–2124, doi:10.1126/science.1064034.

Stephens, G. L., and T. D. Ellis (2008), Controls of global-mean precipitation increases in global warming GCM experiments, *J. Clim.*, *21*, 6141–6155, doi:10.1175/2008JCLI2144.1.

Takahashi, K. (2009), The global hydrological cycle and atmospheric short-wave absorption in climate models under CO_2 forcing, *J. Clim.*, *22*, 5667–5675, doi:10.1175/2009JCLI2674.1.

Williams, K. D., W. J. Ingram, and J. M. Gregory (2008), Time variation of effective climate sensitivity in GCMs, *J. Clim.*, *21*, 5076–5090, doi:10.1175/2008JCLI2371.1.

Yang, F., A. Kumar, M. E. Schlesinger, and W. Wang (2003), Intensity of hydrological cycles in warmer climates, *J. Clim.*, *16*, 2419–2423, doi:10.1175/2779.1.

T. Andrews and P. M. Forster, Institute for Climate and Atmospheric Science, School of Earth and Environment, University of Leeds, Leeds LS2 9JT, UK. (t.andrews@see.leeds.ac.uk)

N. Bellouin, O. Boucher, and A. Jones, Met Office Hadley Centre, FitzRoy Road, Exeter EX1 3PB, UK.